International Journal of Concrete Structures and Materials
Vol.18, No.3E, pp.183~189, December 2006

J-Integral Evaluation of Concrete Fracture Characteristics

Sin-Ho Choi[1], Hae-Ju Kye[2], and Wha-Jung Kim[3]

(Originally published in Korean version of ***Journal of KCI***, Vol.13, No.4, August 2001)

Abstract: Many researchers have recently proposed various parameters, variables of models and experimental methods to evaluate fracture properties of concrete, and their developments allow us to analyze the non-linear and quasi-brittle fracture mechanisms. This paper presents a brief treatment of the fracture parameters. Additionally, three-point bending tests were conducted to compare J-integral (J_{Ic}) with other parameters(K_{Ic}, G_{Ic}, and G_F). The change in parameter values with respect to the width and notch length of concrete beam specimens was also considered. The load-displacement curves were used to measure the concrete fracture toughness experimentally. From the results of experiment, it was found that the value of G_F and J_{Ic} decreased as the notch depth increased and that G_F was less sensitive than J_{Ic}. Therefore, the former, G_F, is more appropriate in using it as the concrete fracture toughness parameter. The values of G_F and J_{Ic} increased when the width of concrete specimens increasing from 75 mm to 150 mm. Thus, the effects of the specimen width should be considered in determining the fracture toughness of concrete.

Keywords: 3-point bending test, fracture parameters, notch length, J-integral, concrete fracture toughness

1. Introduction

Many models and theories, which can analyze the brittle fracture and non-linear (with respect to the strain) behavior of concrete have recently been reported owing to the development of fracture dynamics. Among those widely used models are fictitious crack model, 2-parameter model, size-effect model, etc. Nevertheless, these models assume linear crack tip and ignore the three-dimensional aspect of actual concrete structures to a certain extent. Thus, although the existing fracture dynamics models have successfully described the fracture behavior of concrete structures so far, there are some limitations. One of the limitation is they can not satisfactorily explain the fracture mechanisms of the concrete with respect to its width.

Griffth[1] was the first researcher to work on the fracture phenomenon due to the occurrence and growth of the crack. His theory of brittle fracture explained the occurrence of unstable propagation of crack in completely brittle materials using energy release rate in 1920. His theory of brittle fracture dynamics was applied and developed mainly for metal materials. Kaplan[2] was the first to apply this theory of fracture dynamics to composite cement materials. Many of the earlier researches on concrete fracture dynamics were based on the parameters of fracture dynamics established from the investigation of metal materials. Lott et al.[3,4] measured K_{Ic} and G_{Ic} from their experiments on notched beams and found that there was micro-crack zone at the tip of the crack. In addition, Walsh[5] suggested that the micro-crack zone at the tip of the crack should be smaller than the specimen size and the length of the ligament and that the height of the beam should be at least 150 mm for the concrete fracture experiment. Entering the age of late 1970's, it was widely recognized that the direct application of fracture dynamics for metal materials to concrete was not possible, if not practical, because the softening area was found at the front of crack tip of the concrete, although the tip was damaged, to make the transfer of the stress. Hillerborg[6] proposed a fictitious crack model (FCM), and this model requires factors for stress-crack opening displacement (f_t-COD) obtained from uni-axial tensile strength test and the fracture energy, G_F, obtained from the load-displacement curve of three-point bending test of a beam. Jenq and Shah[7] proposed a two-parameter model based on the elastic fracture response and suggested the characteristic length of a material, Q, which can be expressed by coefficient of stress expansion (K_{Ic}^s) and crack-tip opening displacement ($CTOD_c$). Bazant and Cedolin[8] proposed a crack line model based on the softening of deformation in order to explain the fracture process of the concrete and computed the fracture energy from crack resistance curve (R-curve). Shah and Hamm[9] showed that the fracture behavior of the concrete specimen with notched ends was influenced by the width of the specimen in their tensile strength experiment on the rectangular concrete specimen. The cracks on the concrete exist at the non-linear zone, called fracture process zone (FPZ), from the concrete crack tip, and this zone is formed mainly by the micro-cracks at the tip. Because these micro-cracks exert a very significant influence on the stress distribution at the crack tip, non-linear fracture mechanics

[1] Dept. of Architectural Engineering, Kyungpook National University, Taegu 702-701, Korea. *E-mail: cino@kebi.com*
[2] Hyundai Engineering & Construction Co., Ltd., Seoul 110-793, Korea.
[3] Dept. of Architectural Engineering, Kyungpook National University, Taegu 702-701, Korea.

rather than the traditional linear fracture dynamics is being applied and developed.

This study subjected the test specimens of notched concrete beam to three-point bending test in order to investigate the influence of the change in concrete beam on the concrete fracture toughness. Additionally, the critical J-integral value was compared with other values indicating the fracture toughness.

2. Preparation of the test specimen and experimental method

2.1 Materials and test specimen

This experiment used domestic type I ordinary Portland cement, sand from Yecheon River of Gyungbuk province, crushed stone aggregate from Mt. Pyungeun, and lignosulphonate-based standard AE water reducing agent (reducer) as an admixture. The physical properties of the used materials are shown in Tables 1 and 2. The mix proportion of the concrete used in this experiment is shown in Table 3.

The size of the specimen for the concrete fracture test was set to be the same as the rectangular beam specimen used for previous concrete bending test. The test specimens were prepared with various notch lengths and widths as the experimental variables. The lengths of the notch were set at 0, 25, 50, and 75 mm, and the widths of the specimen were varied at 150, 112.5, and 75 mm. Table 4 shows the shape, size, and notation of the specimens. In addition, the breadth of the notch was set to 5 mm in accordance with the guidelines for the measurement of fracture energy, which set the breadth of the notch to be at or below 10 mm, as specified by the RILEM[10] committee.

2.2 Test method

The screw jack of the loading device was made to maintain the speed of 1 mm/min by the motor rotating at a constant, and the loading device had a maximum allowed capacity of 20 tonf.

Because the measuring of vertical displacement is affected greatly by the local destruction at the contact point of the loading device and the specimen,[11] a frame for measuring the displacement was fabricated as shown in Fig. 1(a). The measurement of vertical displacement was measured at three locations-the deflection at the center point (VT2) and 100 mm left and right of the center point (VT1 and VT3) - by displacement gauge of 1.0 precision. However, only the deflection measurement taken at the center point (VT2) was used for the analysis of the experimental result. Additionally, the crack mouth (opening) displacement (CMOD) was measured by clip gauges of 5.5 precision at both ends (CM1, CM2) from the beam span center in the width-direction (Fig. 1(b)).

Table 1 Physical properties of cement.

Specific gravity	Fineness (cm^2/g)	Setting time(min)		Compressive strength (kgf/cm^2)		
		Ini.	Fin.	3d	7d	28d
3.15	3,140	225	440	210	280	376

Table 2 Physical properties of aggregates.

Class	Specific gravity	G_{max} (mm)	Unit weight (kg/m^3)	Absorption (%)	F.M.
Fine aggregate	2.58	5	1564	1.05	2.91
Coarse aggregate	2.66	25	1569	0.9	6.49

Table 3 Mix proportion of concrete.

G_{max} (mm)	Slump (cm)	Air (%)	W/C (%)	S/A (%)	Unit weight(kg/m^3)				
					C	S	G	W	AD*
25	9 ± 2	4	55	43	327	750	1025	180	1.64

* AD : Lignosulphonate based AE water reducer, normal

Table 4 Shape, size and notation of specimens.

Shape & size	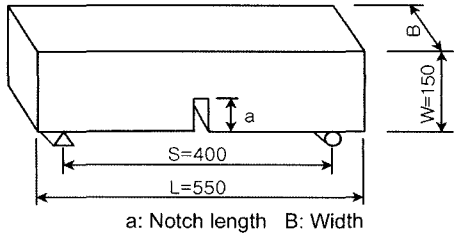 a: Notch length B: Width
Notation	A - ◇◇◇ - ○○ └ Specimen number (01, 02, 03) └ Notch length(00, 25 50, 75) └ Specimen width (A=150, B=112.5, C=75)

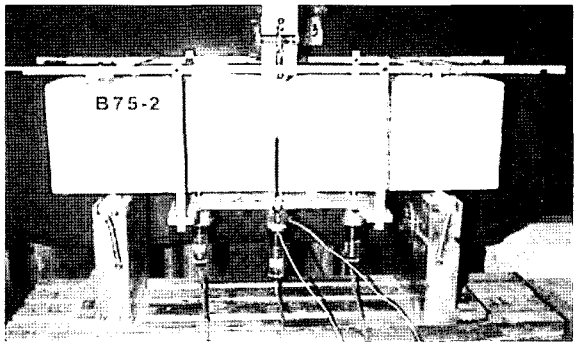

(a) Test set-up

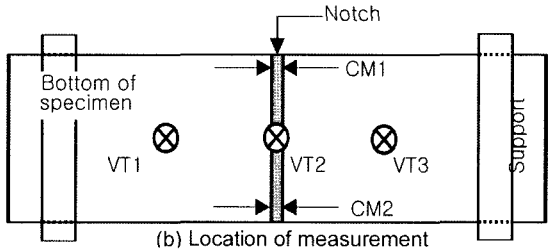

(b) Location of measurement

Fig. 1 Test set-up.

3. Evaluation of material properties of the test specimen

The compressive strength test, tensile strength test, and modulus of elasticity test followed the guidelines of the test methods specified by the Korean (Industrial) Standards, KS F2405, KS F 2423, and KS F 2438, respectively. The result is summarized in Table 5.

The material properties of the specimen tested for the flexural strength were measured, and they included effective flexural strength, coefficient of critical stress expansion, energy release rate, fracture energy and the J-integral value. The results are

Table 5 The property value of compressive test specimens.

Specimen	C.S. (kgf/cm^2)	T.S. (kgf/cm^2)	E (kgf/cm^2)
A	293	25.4	2.59×10^5
B	285	24.4	2.51×10^5
C	301	24.1	2.55×10^5

C.S. : Compressive strength, T.S. : Tensile strength

summarized in Table 6, and the computational method for each item is given as follows.

① Effective flexural strength : The effective flexural strength is calculated from the following relationship among effective cross sectional area at the center of the measured specimen, the flexural moment, and the flexural stress.

$$\sigma_{net} = \frac{3L_pS}{2B(W-a)^2}(three\text{-}point\ bending\ test) \quad (1)$$

W: height, B: width, a: notch length,
S: breadth of the specimen, Lp: Peak load.

② Coefficient of critical stress expansion (K_{Ic}): Assuming that linear fracture dynamics can be applied, the coefficient of critical stress expansion is given as follows.

$$K_{Ic} = Y\sigma\sqrt{\pi a} \quad (2)$$

Y : the coefficient determined from the shape of the test specimen, σ : official flexural strength computed for maximum load assuming there is no notch in the specimen ($\sigma = 1.5L_pS/BW^2$)

Although the S/W for the test specimen used in this study is approximately 2.7 (S/W ≒ 2.7), this study applied the following equations based on the generally known value of 2.5 for S/W ($S/W = 2.5$) because of the difficulty in obtaining the Y value for S/W value of 2.7.

Table 6 Fracture properties of notched beam specimens.

Specimen	a(cm)	B(cm)	(a/W)	Y	E(GPa)	L_p(kN)	δ_p(mm)	σ_{net}(MPa)	σ(MPa)	K_{Ic}(MPam$^{1/2}$)	G_{Ic}(N/m)	G_F(N/m)	J_{Ic}(N/m)
A-00-01	0	15.00	0.00	1.00	25.4	24.40	0.026	4.34	4.34	-	-	-	-
A-00-02	0	15.00	0.00	1.00	25.4	21.29	0.050	3.79	3.79	-	-	-	-
A-00-03	0	15.00	0.00	1.00	25.4	-	-	-	-	-	-	-	-
A-25-01	2.5	15.00	0.17	0.91	25.4	12.76	0.058	3.27	2.27	0.577	13.10	182	80.5
A-25-02	2.5	15.00	0.17	0.91	25.4	11.13	0.052	2.85	1.98	0.503	9.97	178	74.0
A-25-03	2.5	15.00	0.17	0.91	25.4	11.18	0.050	2.86	1.99	0.506	10.07	175	71.8
A-50-01	5	15.00	0.33	0.98	25.4	10.33	0.044	4.13	1.84	0.714	20.09	162	67.2
A-50-02	5	15.00	0.33	0.98	25.4	9.36	0.046	3.75	1.66	0.648	16.52	157	46.9
A-50-03	5	15.00	0.33	0.98	25.4	8.88	0.042	3.55	1.58	0.614	14.87	156	44.3
A-75-01	7.5	15.00	0.50	1.30	25.4	4.94	0.046	3.51	0.88	0.552	12.00	118	30.6
A-75-02	7.5	15.00	0.50	1.30	25.4	5.71	0.058	4.06	1.01	0.638	16.03	146	57.2
A-75-03	7.5	15.00	0.50	1.30	25.4	5.36	0.068	3.81	0.95	0.599	14.11	133	55.6
B-00-01	0	11.25	0.00	1.00	24.6	20.91	0.038	4.96	4.96	-	-	-	-
B-00-02	0	11.25	0.00	1.00	24.6	19.47	0.040	4.61	4.61	-	-	-	-
B-00-03	0	11.25	0.00	1.00	24.6	19.31	0.020	4.58	4.58	-	-	-	-
B-25-01	2.5	11.25	0.17	0.91	24.6	10.39	0.027	3.55	2.46	0.626	15.95	156	58.3
B-25-02	2.5	11.25	0.17	0.91	24.6	10.39	0.022	3.55	2.46	0.627	15.96	161	56.5
B-25-03	2.5	11.25	0.17	0.91	24.6	11.48	0.048	3.92	2.72	0.692	19.48	184	73.6
B-50-01	5	11.25	0.33	0.98	24.6	7.41	0.026	3.95	1.76	0.683	18.98	135	59.7
B-50-02	5	11.25	0.33	0.98	24.6	7.44	0.046	3.97	1.76	0.686	19.14	154	50.8
B-50-03	5	11.25	0.33	0.98	24.6	8.53	0.018	4.55	2.02	0.787	25.16	151	52.2
B-75-01	7.5	11.25	0.50	1.30	24.6	5.52	0.046	5.23	1.31	0.822	27.47	139	33.0
B-75-02	7.5	11.25	0.50	1.30	24.6	5.00	0.032	4.74	1.19	0.746	22.60	120	55.1
B-75-03	7.5	11.25	0.50	1.30	24.6	5.19	0.058	4.93	1.23	0.774	24.37	136	43.0
C-00-01	0	7.50	0.00	1.00	25.0	11.16	0.032	3.97	3.97	-	-	-	-
C-00-02	0	7.50	0.00	1.00	25.0	12.44	0.036	4.42	4.42	-	-	-	-
C-00-03	0	7.50	0.00	1.00	25.0	11.22	0.032	3.99	3.99	-	-	-	-
C-25-01	2.5	7.50	0.17	0.91	25.0	7.44	0.040	3.81	2.65	0.673	18.11	145	53.3
C-25-02	2.5	7.50	0.17	0.91	25.0	9.36	0.048	4.79	3.33	0.847	28.69	163	65.5
C-25-03	2.5	7.50	0.17	0.91	25.0	7.79	0.034	3.99	2.77	0.705	19.87	149	42.8
C-50-01	5	7.50	0.33	0.98	25.0	4.81	0.034	3.85	1.71	0.666	17.72	137	53.2
C-50-02	5	7.50	0.33	0.98	25.0	4.91	0.024	3.93	1.74	0.679	18.43	130	47.8
C-50-03	5	7.50	0.33	0.98	25.0	5.19	0.024	4.16	1.85	0.719	20.66	149	65.0
C-75-01	7.5	7.50	0.50	1.30	25.0	3.55	0.046	5.05	1.26	0.795	25.25	117	35.1
C-75-02	7.5	7.50	0.50	1.30	25.0	3.62	0.040	5.15	1.29	0.810	26.25	106	27.9
C-75-03	7.5	7.50	0.50	1.30	25.0	3.59	0.060	5.11	1.28	0.803	25.79	122	27.1

$$Y = \frac{1.0 - 2.5\alpha + 4.49\alpha^2 - 3.98^3 + 1.33\alpha^4}{(1-\alpha)^{3/2}},\ \alpha = a/W$$

③ Energy release rate (G_{Ic}) : The energy release rate (G_{Ic}) is a potential energy per unit area, which is released when the crack progresses. It is computed indirectly from the values of K_{Ic} and E'. In this study, the energy release rate was computed with the assumption of plane stress condition ($E' = E$). If the specimen is in plane deformation condition, the value of E' is replaced by $E / (1 - \nu^2)$.

$$G_{Ic} = \frac{1}{E'} K_{Ic}^2 \tag{3}$$

where, $E' = E$ (plane stress condition)
$= E/(1-\nu^2)$ (plane deformation condition)
and, E : modulus of elasticity ν : Poisson's ratio

④ Fracture energy (G_F) : The fracture energy is computed by dividing the area under the load-displacement curve by the fractured area (A), and the area under the curve can be calculated by integral calculus.

$$G_F = \frac{U}{A} \tag{4}$$

Here, the influence of the weight of the test specimen on the computation of K_{Ic} and G_F was ignored, for the breadth of the specimen at the point of contact was relatively short.

⑤ Computation of J-integral

Rice et al.[12] proposed a non-analytical evaluation method of J-integral analysis for the test specimens with relatively deep crack, of which the fracture energy is mainly based on the load-displacement curve and is also dependent on the pure cross section (bound by the overall height of the beam to the ligament length). In other words, when the flexural deformation is the dominant case, the value of critical J-integral must be computed by the area under the load-displacement curve to the initial crack point in order to reflect the J-integral value at the starting point of the stable growth of the crack. Okada et al.[13] reasoned that the major crack in regular concrete started at the point of maximum load and explained that the critical J-integral value could be quantified at the point of maximum load. The advantages of the simplified equation proposed by Rice et al. are that the P-δ curve obtained from experiment is applied directly and that J-integral can be evaluated with only one P-δ curve (Fig. 2).

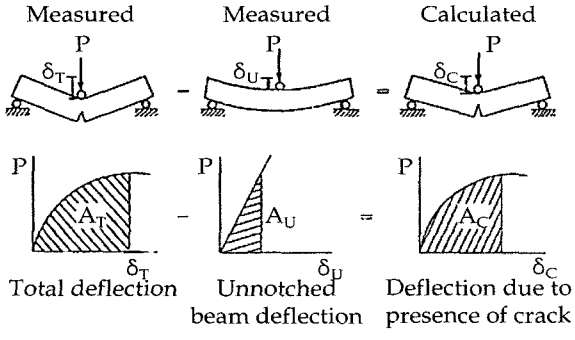

Fig. 2 Experimental decision of J_{Ic}(by Rice & Paris).

$$J = \frac{2}{B(W-a)} \int_0^{\delta_{max}} P \cdot d\delta_C$$

$$= \frac{2}{B(W-a)} (A_T - A_U)$$

$$= \frac{2}{B(W-a)} A_C \tag{6}$$

where, B : width of the specimen δ_{max} : maximum displacement at the loading point

W-a : length of ligament A_U : components not related to th notch

A_T : total potential energy A_C : potential energy due to the notch

4. Experimental result

The load-deflection relationship and load-crack opening displacement relationship are depicted in Figs. 3 and 4, respectively. The graphs illustrate the representative experimental results.

Figs. 5~7 illustrate the relationship of the coefficient of critical stress expansion (K_{Ic}), critical J-integral value (J_{Ic}), and fracture energy (G_F), respectively, to relative notch length.

Figs. 8~10 show the change in K_{Ic}, J_{Ic}, and G_F with respect to the change in the beam width.

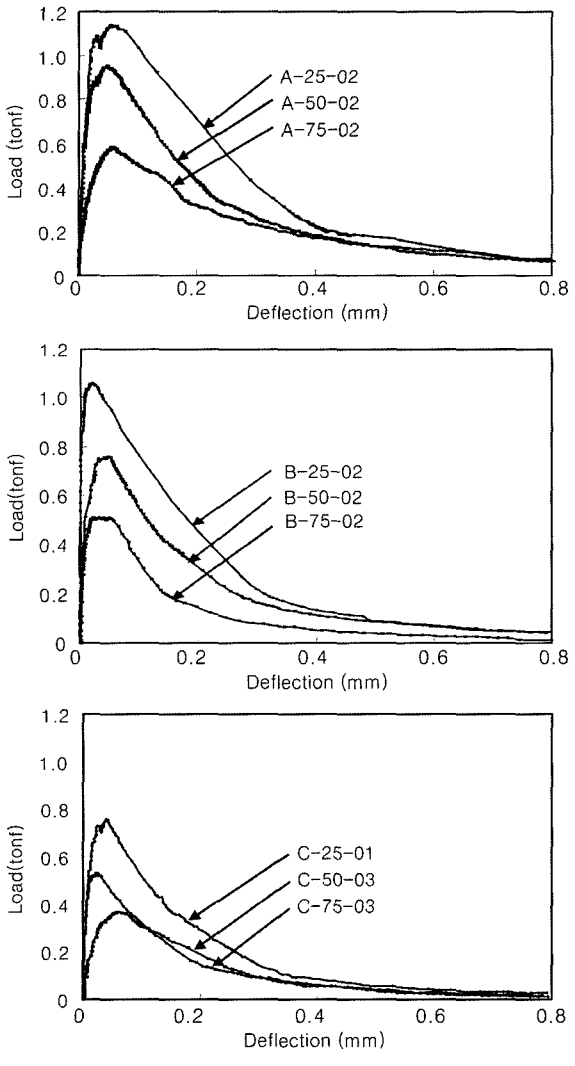

Fig. 3 Load-deflection curve at the center of beam.

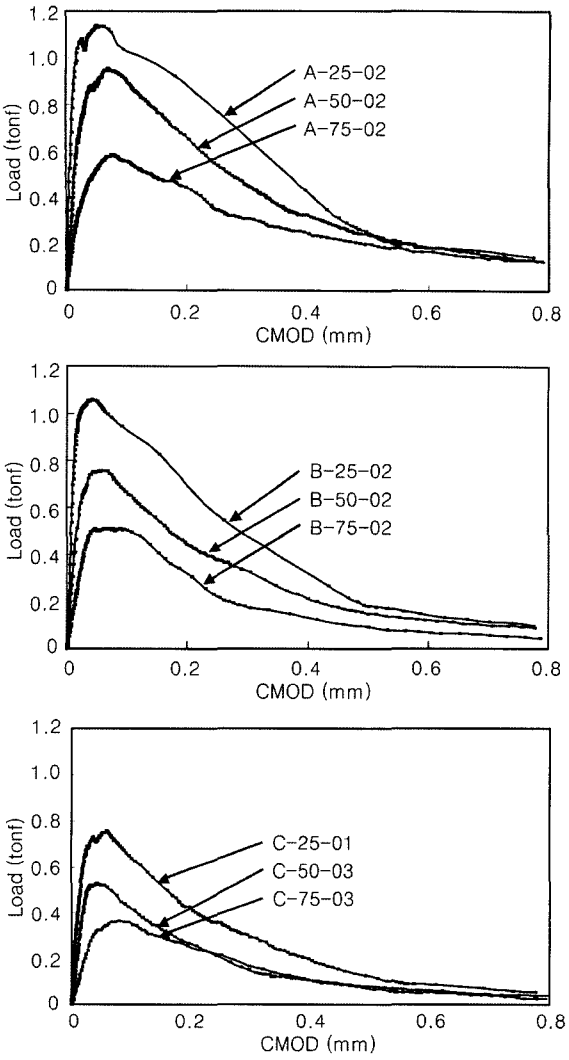

Fig. 4 Load-CMOD curve at the center of beam.

4.1 Comparison of G_F and G_{Ic}

The reason why G_F and G_{Ic} show a big difference in Table 6 is because the scope or range to compute the values is different. In other words, G_F considers the entire range of total energy required to fracture the specimen into two parts, and G_{Ic} considers the elastic energy at the time when the crack progresses to a micro-length. Because the concrete requires a large energy for the propagation of crack and the micro-crack does not amount to a fracture, the fracture energy is more useful than the energy release rate as an indicator of fracture toughness.

4.2 Notch length and fracture energy

The relationship between notch length and fracture energy (G_F) is that the fracture energy tends to increase as the notch length is shorter. This is mainly due to the effect of engagement of the notch with coarse aggregate right after the crack progress because of the complex crack propagation route and the increased possibility for the notch to encounter coarse aggregate as the notch length is shorter and the length of ligament is longer. It was determined that the specimen with longer ligament length had a greater resistance to fracture even the vertical displacement at the center of the loading surpassed 0.5 mm.

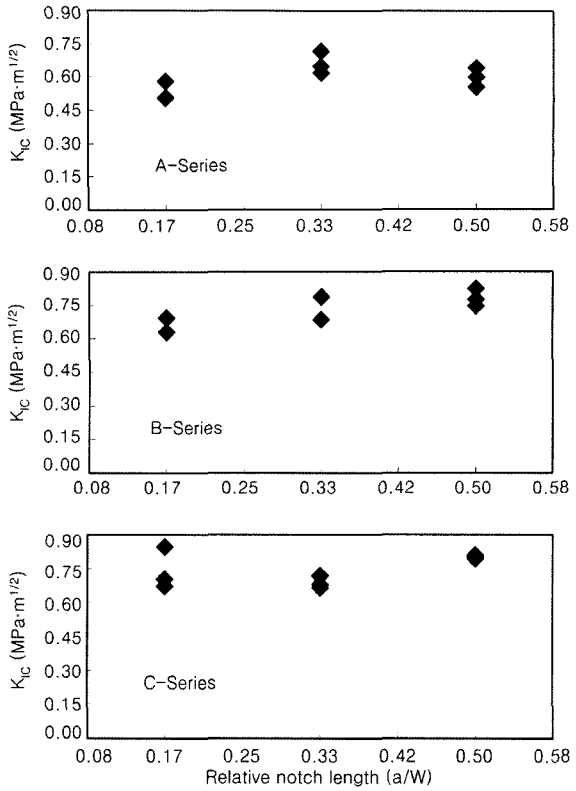

Fig. 5 The relationship of K_{IC} and relative notch length.

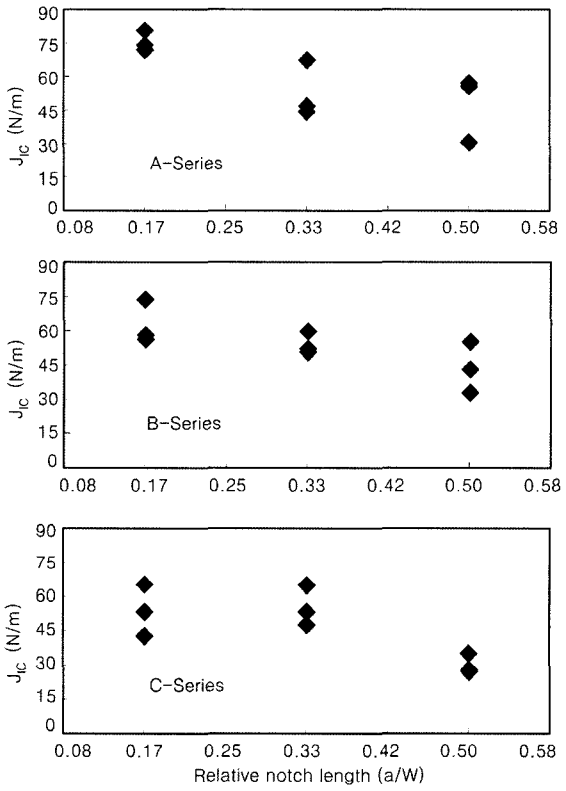

Fig. 6 The relationship of J_{IC} and relative notch length.

4.3 Effect of the width of test specimen

Previous research on the fracture toughness of rectangular concrete specimen with the notches at the both ends found that the fracture toughness tended to decrease a little by little as the

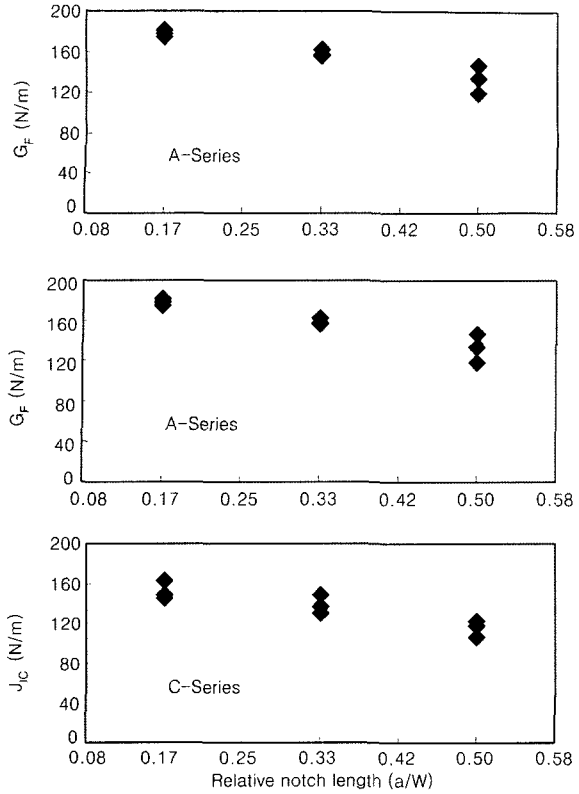

Fig. 7 The relationship of G_F and relative notch length.

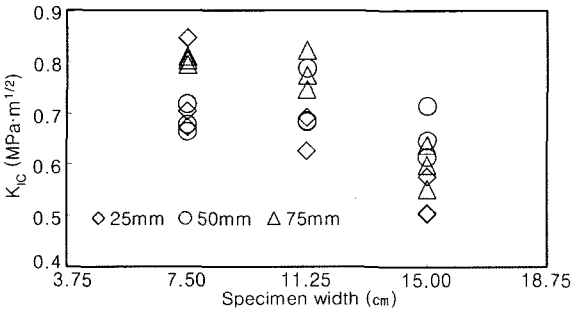

Fig. 8 The relationship of K_{IC} and beam width.

width of the specimen increased. It has been reported that this is due to the brittle nature of the concrete.[9] In this experiment, while the coefficient of critical stress expansion (K_{Ic}) showed the tendency to decrease a little by little as the width of the specimen increased (Fig. 8), the value of the J-integral (J_{Ic}) and fracture energy (G_F) on the contrary showed the tendency to increase linearly with the width of the specimen (Figs. 9 and 10).

This is explained by the fact that the energy required for the crack to propagate increased because the effect of the engagement with the coarse aggregate increased with the increased width of the specimen for all the range of the specimen width. Thus, the effect of the specimen width should be considered in evaluating the fracture toughness of the notched concrete with the crack in progress.

4.4 Comparison of J_{Ic} and G_F

As the notch length increased from 25 mm to 50 mm and 75 mm, the value of J-integral (J_{Ic}) decreased by about 15% and 35%, respectively. In addition, as the width of the specimen was

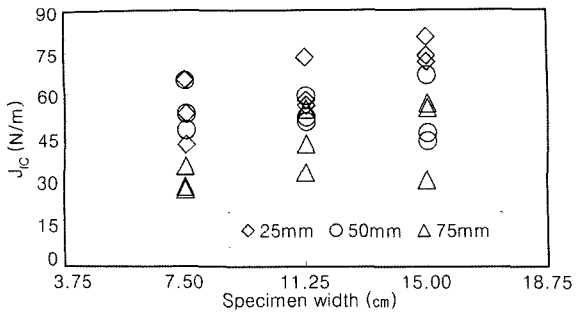

Fig. 9 The relationship of J_{Ic} and beam width.

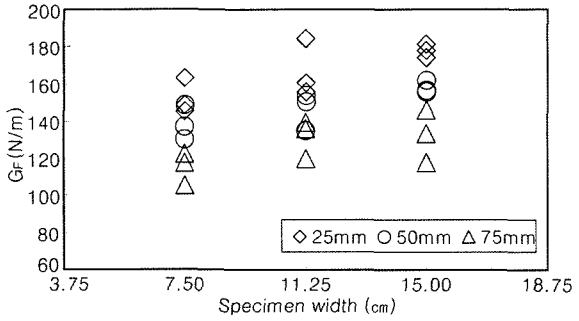

Fig. 10 The relationship of G_F and beam width.

reduced from 150 mm to 112.5 mm and 75 mm, the value of J-integral (J_{Ic}) decreased by about 12% and 24%, respectively. Regarding G_F, the value of G_F deceased by about 10% and 23%, respectively, as the notch length increased from 25 mm to 50 mm and 75 mm. Additionally, as the width of the specimen decreased from 150 mm to 112.5 mm and 75 mm, the G_F value decreased by about 6 % and 12 %, respectively. Thus, it was found that G_F responded less sensitive to the change in notch length compared to the response of J_{Ic} to the change in notch length. This means that G_F is more useful factor in the evaluation of fracture toughness of the concrete based on this experiment. Because the value of J_{Ic} reacts very sensitive to the change in notch length at the maximum load of the experiment, the selection of the maximum load greatly affects the computation of J_{Ic} by the experiment.

5. Conclusions

A three-point bending experiment was carried out in this study to investigate the influence of notch length and specimen width on the fracture toughness of the concrete. The following conclusions are obtained based on the experimental results.

1) The factors of non-linear fracture toughness of the concrete (J_{Ic}, G_F) decreased greatly as the notch length increased. Especially, because the fracture energy (G_F) reacted less sensitive to the change in notch length compared to the response of the J-integral (J_{Ic}) value, the fracture energy (G_F) is deemed to be a more useful factor compared to the J-integral (J_{Ic}) in evaluating the fracture toughness in response to a change in notch length.

2) Because the critical J-integral value (J_{Ic}) and fracture energy (G_F) tended to increase as the width of the concrete

specimen increased from 75 mm to 150 mm and 112.5 mm in between, the effect of specimen width should be definitely considered in the evaluation of the fracture toughness of the concrete.

3) This study should be followed by a research on numerical analysis methods of the J-integral and the scope, to which the J-integral can be applied.

References

1. Griffith, A. A., *The Phenomena of Rupture and Flow in Solids*, Philosophical Transactions of the Royal Society of London, Series A 221, 1920, pp.163~198.

2. Kaplan, M. F., "Crack Propagation and Fracture of Concrete," *Journal of the American Concrete Institute*, Vol. 58, No. 5, 1961, pp.591~610.

3. Lott, J. L. and Kesler, C. E., "Crack Propagation in Plain Concrete," *Symposium on Structure of Portland Cement Paste and Concrete*, 1966, pp.204 ~218.

4. Lott, J. L., Kesler, C. E., and Naus, D. J., "Fracture Mechanics Its Applicability to Concrete," *Mechanical Behavior of Materials*, Vol.4, 1972, pp.113~124.

5. Walsh, P. F., "Crack Initiation in Plain Concrete," *Magazine of Concrete Research*, Vol.28, No.94, 1976, pp.37~41.

6. Hillerborg, A., Modeer, M., and Petersson, P. E., "Analysis of Crack Formation and Crack Growth in Concrete by Means of Fracture Mechanics and Finite Elements," *Cement and Concrete Research*, Vol.6, 1976, pp.773~782.

7. Jenq, Y. S. and Shah, S. P., "A Two parameter Fracture Model for Concrete," *Journal of Engineering Mechanics*, Vol. 111, No.10, 1985, pp.1227~1241.

8. Bazant, Z. P., Cedolin, L., "Blunt Crack Bond Propagation in Finite Element Analysis," *Journal of Engineering Mechanics*, ASCE, Vol.105, No.2, 1979, pp.297~315.

9. Shah, S. P., Hamm. J., and Ouyang, C, "The Effect of Specimen Thickness on Fracture Behaviour of Concrete," *Mag. of Concrete Research*, No.175, 1996, pp.117~129.

10. RILEM Committee on Fracture Mechanics of Concrete-Test Methods, "Determination of the Fracture Energy of Mortar and Concrete by Means of Three-Point Bend Tests on Notched Beams," *Materials and Structures*, Vol.18, No.106, 1985, pp.285~290.

11. Kim S. G, "Relationship of Crack Opening Displacement and Displacement in Loading Direction of Concrete," *Journal of Korea Concrete Institute*, Vol.9, No.1, 1997, pp.183~194.

12. Rice, J. R., Paris, P. C., and Merkle, J. G, *Some Further Result of J-integral Analysis and Estimate in Process in Flaw Growth and Fracture Toughness Testing*, ASTM STP, 536, 1973, pp.213~245.

13. 岡田 清, 小柳 治, 六郷惠哲, "コンクリートの曲げ引張 破壞過程に關するエネルギ?的考察," 日本土木學會論文報告集, 第285卷, 1979, pp.109~119.